Effect of Chemical Modification on Macroscopic Phase Separation in Styrene−Isoprene Block Copolymer Driven by Thermooxidative Reactions

Shaobin Fan[†] and Thein Kyu*

Institute of Polymer Engineering, The University of Akron, Akron, Ohio 44325

Received October 22, 2003; Revised Manuscript Received December 5, 2003

ABSTRACT: Macroscopic phase separation induced by thermooxidative reaction has been observed in a commercial styrene-*block*-isoprene-*block*-styrene (SIS) copolymer, Kraton 1107, upon exposure to atmospheric oxygen at elevated temperatures. Unlike styrene-*block*-butadiene-*block*-styrene (SBS) copolymers, there is essentially no gel formation (i.e., no cross-linking reaction) in the thermal oxidation of SIS copolymer. In the first phase separation, oxidative reaction causes the breakup of the SIS triblock chains into the SI blocks (containing polystyrene blocks and short isoprene segments) and low molar mass neat polyisoprene, forming an immiscible region with macrophase-separated domains. The continued decline of the molecular weight of polyisoprene and further detachment of isoprene fragments from the SI diblocks suppress the immiscibility region to a lower temperature, causing phase dissolution to occur at the reaction temperature. With progressive oxidation, the chain scission continues to occur while heavily oxidized lower molecular weight polyisoprene derivatives and oily byproducts are formed. Such chemical change in polyisoprene makes the system to be very unstable, thereby driving the macroscopic phase separation for a second time. It may be concluded that the cascading phase separation occurs due to chemical modification of the isoprene units of the SIS blocks as opposed to the cross-linking reaction induced macrophase separation in the SBS blocks.

Introduction

Phase transition and structure formation in block copolymers have attracted immense attention from both academia and industries. By virtue of the repulsive force among chemically joined blocks, a block copolymer tends to self-assemble to an ordered state in approaching the equilibrium. Such a self-organized structure typically has a characteristic length of tens to a few hundreds of nanometers, depending on chemical structure/composition, molecular weight, and block ratio. Well-known microstructures include spherical, cylindrical, gyroid, and lamellar domains at equilibrium.[1−5] In addition, the morphology and domain size of a block copolymer may be governed by chemical and physical parameters such as chemical interaction, temperature, pressure, and mixing conditions. Recently, while there have been considerable advances on amphilphilic block copolymers with potential applications such as drug delivery and surfactants,[6−8] block copolymers consisting of hard and soft segments remain the most important ones due to their combined excellent mechanical properties and good processability. More importantly, such a block copolymer can be designed and tailored to meet property requirements in the forms of thermoplastic elastomers and/or toughened plastics.

Among block copolymers, styrene-*block*-isoprene-*block*-styrene (SIS) and styrene-*block*-butadiene-*block*-styrene (SBS) copolymers were the first to be commercialized and also most widely used. These copolymers have relatively high molecular weights and possess microphase-separated structure at room temperature. Such an ordered structure becomes homogeneous at an elevated temperature, often called order−disorder transition temperature, T_{ODT}. To process SIS and SBS block copolymers into final products, the processing temperature is desirable to be higher than T_{ODT} but lower than the thermal degradation temperature to avoid chain rupture. In practice, commercial SIS and SBS block copolymers have been processed at temperatures in excess of 200 °C. Such a high processing temperature exerts a profound effect on the structure and properties of SIS and SBS block copolymers. Hence, phase behavior and structural stability of these materials at elevated temperatures are of paramount importance for practical applications.

It is well documented that most unsaturated polymers are susceptible to oxygen attack, particularly at high temperatures.[9−13] In fact, thermooxidative reactions have been regarded as the main reason for the deterioration of polydiene and its products during service. Such effect is particularly pronounced in rubbers or polymers with unsaturated bonds such as dienes.[9−13] Therefore, it is natural to infer that block copolymers consisting of isoprene or butadiene blocks are vulnerable to the oxygen attack, particularly at elevated temperatures in air. An important question is how thermal oxidation affects the microstructure of SIS and SBS block copolymers. Although microscopic phase separation and ordered structure in styrene−isoprene and styrene−butadiene block copolymers have been investigated extensively, studies on phase behavior and structure development of block copolymers upon exposure to atmospheric oxygen at elevated temperatures are rare. Since oxidation is known to be a serious problem in SIS and SBS block copolymers during mixing and molding,[14] it is essential to understand the phase behavior and morphology of these block copolymers under practical thermooxidative conditions.

Although there are few reports on thermal oxidation of styrene−isoprene block copolymers at elevated tem-

[†] Current address: ZMS, LLC, 5764 Shellmound Street, Emeryville, CA 94608.

* To whom correspondence should be addressed.

10.1021/ma0355960 CCC: $27.50
Published on Web 01/17/2004

perature, extensive research hitherto has been carried out on oxidation in neat polyisoprene. Such investigation was initiated nearly a century ago to explain why and how oxidation affected rubber elasticity. Since then, thermooxidation has been recognized as one of the most important processes for the deterioration of rubber products. All rubbers made from diene monomers are highly susceptible to oxidative degradation due to the presence of an allylic group in the polymer backbone. Repeated double bonds in a hydrocarbon chain, e.g., polyisoprene, increase the rate of oxidation about 30 times in comparison to a fully saturated chain. Temperature and oxygen levels thus play an important role in oxidative reactions of rubbery materials.

Recognizing the possible degradation of polyisoprene and polybutadiene blocks, researchers have paid careful attention to experiments that involve styrene−isoprene and styrene−butadiene block copolymers. For examples, vacuum-sealing of samples[15] or low processing temperatures[16,17] have been employed to prevent degradation of styrene−isoprene and styrene−butadiene block copolymers. However, there remain cases in which thermal oxidation cannot be completely avoided. It is, therefore, of particular interest to investigate the degradation behavior of these block copolymer subjected to harsh conditions.

In previous publications,[18] we reported the observation of macroscopic phase separations in a styrene-*block*-butadiene-*bloc*k-styrene copolymer (Kraton 1102, Shell Chemical Co., now Kraton Business Group) and two as-synthesized styrene-*block*-butadiene and styrene-*block*-butadiene-*block*-styrene copolymers at elevated temperatures in an atmospheric environment.[18] All three styrene−butadiene block copolymers exhibited similar phase-separated structures upon heating in open air, regardless of the difference in molecular weight and copolymer architecture. The macroscopic domains grew rapidly in the early stage, then phase dissolution occurs in competition with the first phase separation, and a cascading second phase separation emerged at a later time. It was shown that the macroscopic phase separation originated from the thermooxidative reactions involving chain scission and cross-linking reactions. Moreover, chain scission is the predominant reaction in the early stage of the macroscopic phase separation whereas cross-linking becomes dominant at a later time.

In the present paper, phase behavior and structural development in a styrene−isoprene block copolymer (Kraton 1107) were investigated by means of optical microscopy, time-resolved light scattering, thermal analysis, gel permeation chromatography (GPC), and gel content measurements by exposing the sample to air at elevated temperatures. To understand the behavior of styrene−isoprene block copolymer under processing conditions, experiments were undertaken at a constant heating rate and an isothermal condition. Complex macroscopic phase transitions were observed in both the heating cycles and isothermal processes. A possible mechanism for such complex phase separation process is proposed.

Experimental Section

A commercial styrene-*block*-isoprene-*block*-styrene copolymer (Kraton 1107) was used in this work. The block copolymer was kindly provided by Shell Chemical Co. The molecular characteristics of the blocks are 10000 S−110000 I−10000 S, where S represents styrene block and I denotes isoprene block. Note that the SIS triblocks in K1107 were prepared by coupling the two SI diblock units, and thus K1107 contained some residual 20% SI diblock copolymers. For light scattering and optical microscopy experiments, these block copolymer samples were prepared by first dissolving Kraton 1107 in toluene to obtain 5% w/w solution, and then two aliquots of the solution were spread on a glass slide to form a thin film with a thickness ca. 10 μm. All samples were left in open air overnight before putting them in a vacuum oven for 1 day at room temperature, followed by 24 h at 50 °C. The drying temperature was further raised to 80 °C, and samples were dried for 12 h; the final drying was conducted at 110 °C for 1 h under vacuum. The samples for thermal analysis were prepared following a similar procedure; however, the thickness of the films was much larger, ca. 0.5 mm.

The optical microscope (OM) used in this work was from Nikon Corp. (model Optiphot-2). A hot stage (Mettler, model FP82HT) was utilized for a precise temperature control within ±0.1 °C. A Nikon camera was mounted on the top of the microscope and was connected to an exposure controller (model UFX-DX, Nikon). Under the bright field, a direct OM observation was made without requiring any contrast enhancing techniques because the refractive index contrast of the macrophase-separated styrene domains and isoprene phase was sufficiently high. OM digital images were collected as a function of elapsed time.

The cloud point measurements were carried out at a fixed angle of 10° for all samples. A randomly polarized 2 mW He−Ne laser source (LSR2R, Aerotech) with a wavelength of 632.8 nm was utilized, and the scattered light intensity was detected by a photodiode (62/3A27, Pacific Instrument). The heating chamber was a brass block and a brass cover equipped with a thermocouple and two heating rods connected to a temperature controller (Omega, model 2010). The heating rate was 1 °C/min unless indicated otherwise. Time-resolved light scattering experiments were performed in a laser scattering apparatus using a one-dimensional silicon diode Reticon detector (model 1452A, Princeton Applied Research) coupled with an optical multichannel analyzer (model 1460, OMA III, Princeton Applied Research). The scattered light by the sample was projected on an image screen and detected by the Reticon camera. The laser source and heating chamber were the same as those used in the cloud point measurement.

A thermal analyzer (DuPont, model 9900) equipped with a heating cell and a temperature module (model 910) was utilized. The differential scanning calorimetry (DSC) curves of the fresh SIS samples were recorded during isothermal scans at indicated temperatures. The temperature calibration was undertaken based on an indium standard.

Gel permeation chromatography (GPC) equipped with isocratic pump (Waters model 510) and a refractive index detector (model 410) was used in the determination of the molecular weight and distribution of each sample with varying thermal treatment time. Three separation columns with pore sizes of 10^2, 10^3, and 10^4 Å were utilized. The molecular weights and distribution of soluble portion were determined by polystyrene standards. To measure the gel content, samples with or without thermal treatment were refluxed with excess THF for 24 h. The insoluble portion of copolymer was regarded as the gel content, which was found to be absent in the present SIS system.

Results and Discussion

The cloud point plot showing the scattered intensity (at 10°) vs temperature of Kraton 1107 during the course of heating is depicted in Figure 1. The scattered intensity of laser light exhibits a complex variation with temperature, exhibiting two peaks centered at 117 and 126 °C. Above 210 °C, the intensity decreases and gradually levels off. The scattering of light by Kraton 1107 indicates the existence of heterogeneity (or structure) with average domain sizes comparable to or larger than the wavelength of visible light. Although light scattering results alone would be inadequate to deter-

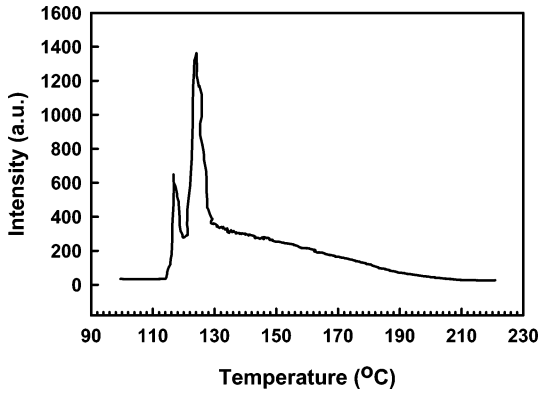

Figure 1. Change of scattered light intensity of Kraton 1107 during the course of heating. The heating rate was 1 °C/min.

mine any mechanism, it may be speculated that the rise and subsequent decay of scattered intensity followed by a second increase may be due to the emergence of some heterogeneous structures, accompanied by phase dissolution and second phase separation.

To gain further insight into the emerging morphology, optical microscope pictures were taken for the Kraton 1107 copolymer as a function of time during heating in air. Figure 2 exhibits the evolution of domain structure of Kraton 1107 during the course of heating. It is worth noting that the picture of the initial copolymer film is featureless, suggestive of a homogeneous structure at least at the optical length scale. However, the micron-sized phase-separated domains emerge at 119.4 °C and grow rapidly. The initial domain structure is, although by no means a proof for spinodal decomposition (SD), reminiscent of a SD-like bicontinuous structure. The SD-like domains grow primarily through coalescence to larger interconnected shapes (122.8 °C) that eventually break down into droplets driven by surface tension. These phase-separated structures tend to disappear within the droplets as well as in the matrix. In the meantime, the size of small droplets inside the larger domains reduces to tiny dots and then disappears (127.2 °C), suggestive of the onset of phase dissolution. Newer small droplets develop again in the matrix at 129 °C, indicating a second macrophase separation, hereafter called "cascading phase separation". A distinct interface of the larger droplets is still discernible in the micrographs; however, this interface fades away (see the picture at 131 °C) as the contrast between the dispersed domains and the matrix diminishes upon prolonged heating. In addition, small droplets appear in the area previous occupied by large domains formed in the first phase separation. The interface of tiny droplets fades away noticeably at 210 °C while the domain sizes seemingly remain the same as that at 140 °C. At 250 °C, polymer degradation becomes very severe, showing burned spots.

To further explore phase behavior and structure development, isothermal experiments were undertaken at a temperature of 160 °C that is below the T_{ODT} of Kraton 1107 but above the oxidative degradation temperature. In Figure 3 is shown the temporal evolution of macroscopic phase separation in Kraton 1107 at 160 °C. The phase transitions under isothermal conditions are similar to that in the course of heating involving first phase separation, phase dissolution, and cascading second phase separation. A spontaneous phase separation emerges from the featureless film to the heterogeneous domains at the heat treatment time of 100 s. These domains tend to diminish due to the reduction of the refractive index contrast and seemingly disappear at 190 °C. A low viscosity in the growing matrix was also observed during the initial phase separation step. Compared to the nonisothermal heating experiment, there are two noteworthy observations. First, the ongoing phase dissolution of the first phase-separated structure is noticeably clear, as evidenced by the diminishing contrast and reduction in domain sizes from 115 to 190 s. Second, a flow pattern is visible at 200 s, suggesting the viscosity reduction along with the reappearance of the smaller domains by virtue of the cascading phase separation.[19]

Time-resolved light scattering experiments were undertaken to mimic the growth dynamics of the phase transitions in Kraton 1107. Figure 4a shows the temporal evolution of the scattered intensity vs scattering vector at the early stages (0−5 s). There is no scattering peak for the starting sample at zero time (note that an induction time of 97 s was subtracted from the total heating time). The first phase separation was evidenced by the appearance of the scattering peak at 10 s that intensified up to 5 s. Subsequently, the scattered intensity decayed from 6 to 23 s, indicating the occurrence of phase dissolution (Figure 4b).

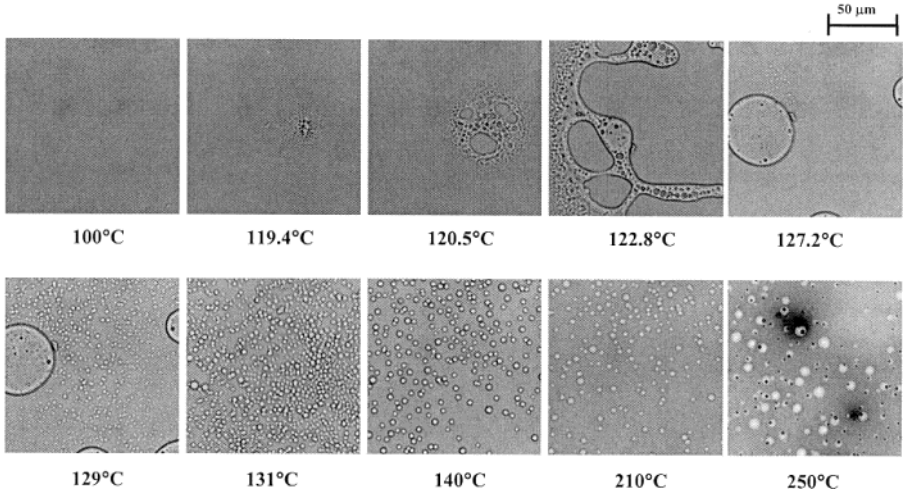

Figure 2. Optical micrographs of temporal evolution of phase transitions of Kraton 1107 during the course of heating. The heating rate was 1 °C/min.

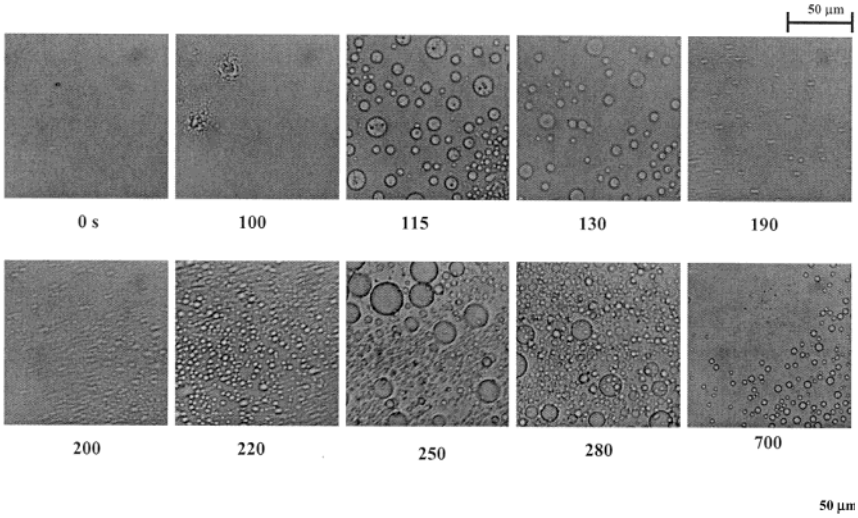

Figure 3. Optical micrographs of temporal evolution of phase-separated morphology of Kraton 1107 subjected to heat treatment at 160 °C.

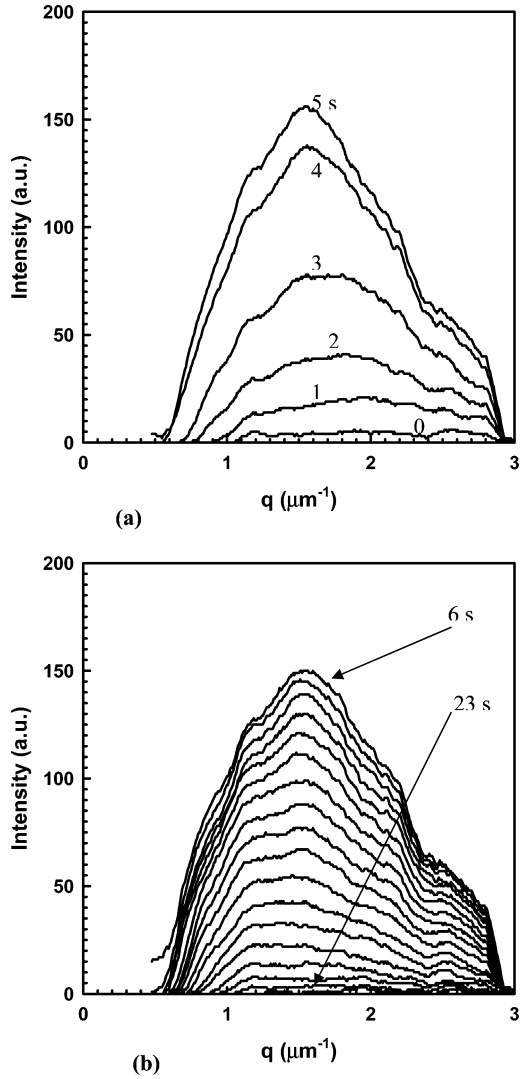

Figure 4. Change of scattered light intensity of Kraton 1107 as a function of scattering vector during the course of (a) first phase separation (0−5 s) and (b) phase dissolution at 160 °C; the scattering curves from the top to the bottom indicate an increment of 1 s from 6 to 23 s.

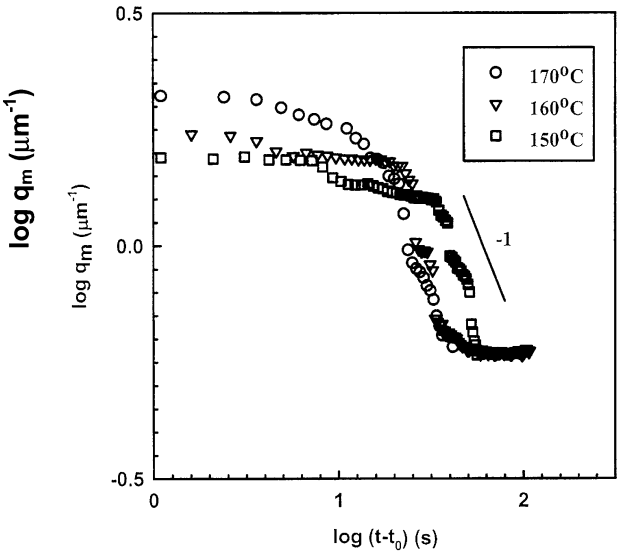

Figure 5. Growth dynamics curves of second phase separation of Kraton 1107 obtained by time-resolved light scattering as indicated temperatures, where t_0 is the induction time. Note that an induction time of 197 s was subtracted from the actual time of annealing.

In Figure 5 are shown the plots of scattering peak (q_m) of the second phase-separated domains as a function of time (t) at different temperatures. The domain size and growth dynamics in the temperature range are consistent with the optical microscopy observations. From the power law plot, i.e., log q_m vs t, the temporal scaling hypothesis[20] ($q_m \sim t^{-\alpha}$) may be tested. As can be seen in Figure 5, the growth curves are by no means linear, showing significant acceleration of domain growth after the initial to intermediate stages. The classical temporal scaling law is evidently not applicable to the entire range of growth in the present macrophase separation. If one approximates the slope in the limited time scale of the late stages, the growth exponent is close to unity, which incidentally corresponds to the hydrodynamic regime similar to the systems undergoing thermally induced phase separation. As evidenced by the wavenumber maxima in the terminal region, the final domain sizes were approximately the same for the three temperatures.

The morphology evolution behavior of Kraton 1107 was also investigated at 150 and 170 °C, but only the results of 150 °C are shown in Figure 6 because the structures and growth dynamics at 170 °C closely

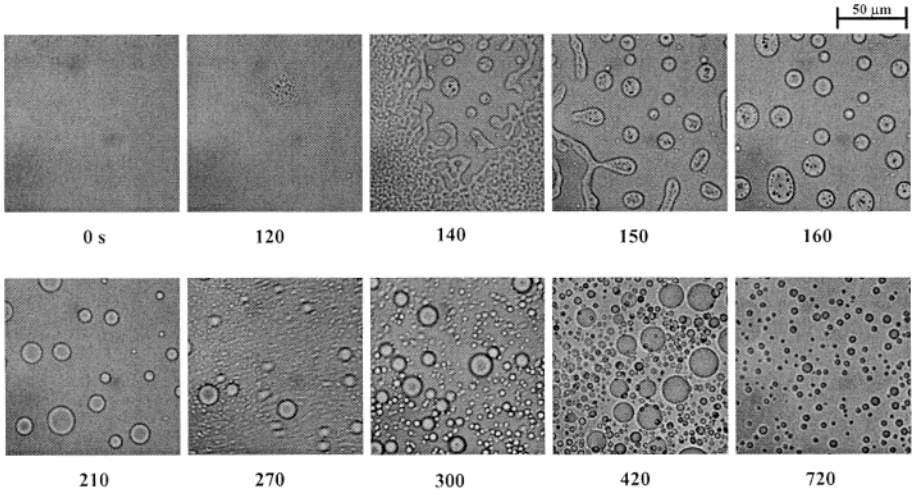

Figure 6. Optical micrographs of temporal evolution of phase-separated morphology of Kraton 1107 subjected to heat treatment at 150 °C.

resemble the micrographs at 160 °C. In the 150 °C case, the phase dissolution process appears different from those of 160 and 170 °C. Although the domain size decreases somewhat, the contrast between the phases formed in the first phase separation does not diminish appreciably before the emergence of cascading phase-separated structure at 270 s, implying the relative competition between the first phase separation and the phase dissolution.

An important question is what kind of phase transitions have been taking place in Kraton 1107. One can rule out the microphase separation because the microdomain structures (a few tens of nanometers) in block copolymers are too small to be detected by light scattering or optical microscopy. Furthermore, the order−disorder transition temperature of Kraton 1107 was reported to be 230 °C,[17] which is significantly higher than the temperature range of 120−170 °C at which phase changes were observed. One possible account is that Kraton 1107 is known to be a mixture of SIS triblock and SI diblock copolymers. That is to say the Kraton 1107 SIS triblock copolymer was synthesized by simply coupling the two SI diblock chains; thus, there remain some 20% residual of the unreacted SI blocks. Therefore, the block copolymer mixture could segregate at elevated temperatures. However, this is unlikely since the mobility of SIS triblock copolymer is limited at temperatures well below T_{ODT}. Also, the refractive index difference between the original triblock and diblock copolymers may not be sufficient to cause scattering of light since the two copolymers have the same block ratio. More importantly, these Kraton 1107 samples containing the mixed SIS/SI are optically clear. All of the above facts indicate that the segregation between SIS and SI block copolymers cannot explain the three-stage complex behavior of the phase transitions. Hence, a more likely scenario for the observed macrophase separation is due to the molecular weight reduction and/or chemical structure alternations resulting from thermal oxidations.

To verify the thermooxidative reactions, isothermal DSC runs of fresh Kraton 1107 samples were undertaken at three different temperatures of 150, 160, and 170 °C. Figure 7 depicts the DSC isotherms of the fresh Kraton 1107 films during exposure to atmospheric environment. In all cases, two exothermic peaks (indicated by the lines) can be discerned, which may be

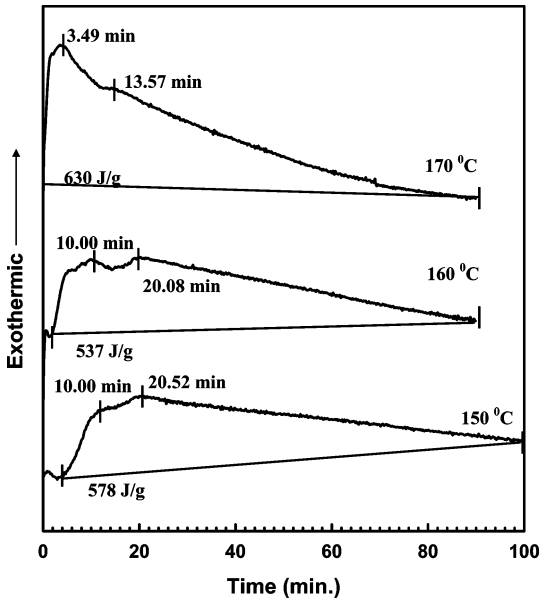

Figure 7. Isothermal DSC scans for a fresh Kraton 1107 sample as a function of heat treatment time at 160 °C.

attributed to thermooxidative reactions since DSC runs under nitrogen flow do not have any detectable heat release or absorption at the same temperatures (data not shown). The dual exothermic peaks imply the existence of two major reactions. As expected, the time for the maximum heat release is expedited with increasing isothermal temperature. At 170 °C, the reaction initiates almost immediately upon heating with a stronger first peak, suggestive of a faster first reaction. Then the two exothermic peaks become comparable having about the same peak height at 160 °C, while the trend reverses as the second peak becomes predominant at 150 °C. A small induction period can be discerned at 160 °C, but it becomes longer at 150 °C. It is worth noting that these exotherms extend beyond 80 min, suggestive of persistent chemical reactions. In addition, the total reaction heat capacity at three temperatures is close to each other, which indicates that the reactions are simply related to the amount of isoprene present.

Since polystyrene is thermally more stable than polyisoprene, the unsaturated double bond of the isoprene segment in Kraton 1107 is likely the place where oxygen attack would occur. One can expect the molec-

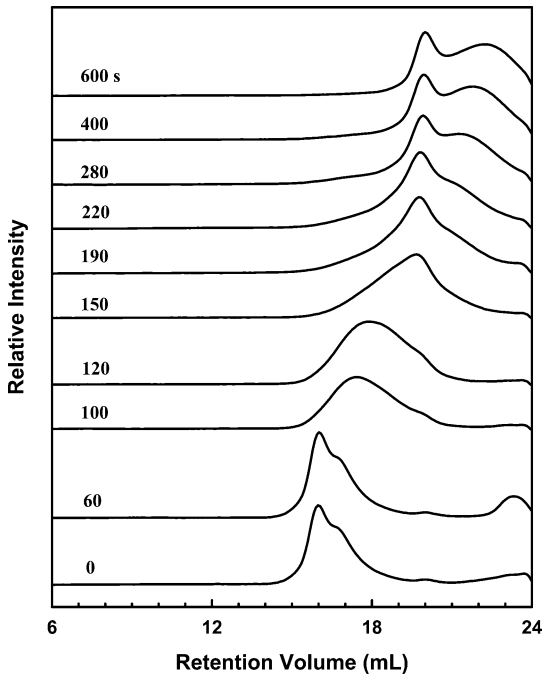

Figure 8. Evolution of GPC traces of a fresh Kraton 1107 sample as a function of heat treatment time. Time zero represents the fresh sample before receiving heat treatment at 160 °C.

Table 1. Molecular Weights and Weight Distributions of Kraton 1107 during Heating at 160 °C

treatment time (s)	M_p (1st peak)	M_p (2nd peak)	M_w	M_n	M_w/M_n
0	224 100		170 200	100 000	1.70
60	204 800		162 300	94 600	1.72
100	72 000		75 100	38 000	1.98
120	54 300		57 400	28 800	1.99
150	14 200		28 800	11 400	2.53
190	13 400		22 300	5 000	4.48
220	12 600		19 100	4 400	4.32
280	11 900	4200	15 200	3 100	4.95
400	11 900	2600	10 200	2 400	4.25
600	11 200	1700	6 000	1 900	3.07

ular weight to decrease with heat treatment time, since chain scission is known to be a dominant reaction in the neat polyisoprene as well as in the styrene−isoprene copolymers. To find out possible chain scission in Kraton 1107, the GPC experiment was carried out for the samples heat-treated at 160 °C. Figure 8 shows the evolution of GPC traces as a function of thermal treatment time for Kraton 1107. Molecular weights and their distributions thus obtained are summarized in Table 1. For a fresh sample, GPC trace exhibits a primary peak at a retention volume of 16 mL and a small shoulder at 16.8 mL. The major peak may be attributed to the SIS triblock molecules while the shoulder peak is probably due to the SI diblock chains. The GPC chromatogram remains essentially the same up to 60 s. However, drastic changes in the GPC trace can be discerned at 100 s. This time corresponds to the emergence of phase-separated domains in Figure 3. It is striking to discern that the original peak and the shoulder change into one broad peak centering at 17.5 mL, with the apparent breakdown of the majority of the SIS triblock and SI diblock chains. The reduction in the peak molecular weight is rather dramatic, from 204 800 to 72 000 within 40 s. Note that a shoulder near 19.8 mL appears at 120 s, which has a peak molecular weight of approximately 14 200 which is slightly higher than the molecular weight of polystyrene block in Kraton 1107. A drastic shift of the peak occurs between 120 and 150 s, in which the molecular weight of the copolymer decreases from 54 300 to 14 200. This peak moves only slightly with the continued heat treatment, i.e., from 19.8 mL at 120 s to 20.0 mL at 600 s, suggesting that most isoprene segments, if not all, may have been detached from the styrene blocks, leaving very little isoprene fragments in the copolymer, if any.

Another important observation is the emergence of a shoulder near 21.7 mL at 190 s. The shoulder becomes a peak at 280 s with a molecular weight of 4200 and broadens with further heat treatment. It should be emphasized that there has been a continuous reduction in high molecular weight fraction and generation of low molecular weight isoprene species since 60 s. At the end of the thermal treatment, effectively all original SIS triblock and SI diblock copolymers have disappeared, as evidenced by the GPC trace at 600 s. Evidently, the polystyrene block remains intact during the thermal treatment. Then the only logical explanation for the abundant low molecular weight products may be the oxidized short polyisoprene segments resulted from the oxidative chain scission reactions. It appears that the isoprene chain becomes shorter due to chain scission while more functional groups such as epoxide, hydroperoxide, etc., are formed in the backbone chains.[21−27] It is reasonable to infer that the concentration of the functional groups per isoprene chain increases with progressive oxidative chain scission.

The plots of molecular weight as a function of thermal treatment time are given in Figure 9. The peak molecular weight exhibits a rapid drop from 60 to 150 s. With the prolonged heat treatment, the peak molecular weight levels off and approaches 11 200, which is very close to 10 000, the original molecular weight of polystyrene block in the Kraton 1107. The molecular weight of the second peak continues to decrease from 4200 at 300 s to 1700 at 600 s, which is very close to the number-average molecular weight of 1750 reported for polyisoprene after 2 h of oxidation at 115 °C. When overall number-average and weight-average molecular weights are considered, continued reduction of the molecular weight is evident with further heat treatment.

As in the case of SBS, the gel content experiments were carried out by dissolving Kraton 1107 samples in THF which were thermally treated at 150, 160, and 170 °C in atmospheric oxygen. The progression of the cross-linking reaction was determined through the measurement of gel content from the undissolved portion of the copolymer in THF for various heat treatment times. No discernible gel was detected for the heat treatment time up to 600 s, suggesting that the cross-linking reaction is absent for Kraton 1107 in the temperature range investigated. This finding is completely different from that of the SBS in which the cascading phase separation is driven by the cross-linking reaction.

It is of interest to estimate the number of chain scissions with heat treatment, which may be calculated by a simple expression under the assumption of random chain scission along the polymer backbone. Let N_S be the number average of scission events per chain experienced by polyisoprene up to time t; then

$$N_S = \bar{X}_0/\bar{X}_t - 1 \qquad (1)$$

where $\bar{X}_0$ and $\bar{X}_t$ are the number-average degree of polymerization of the starting copolymer and that at

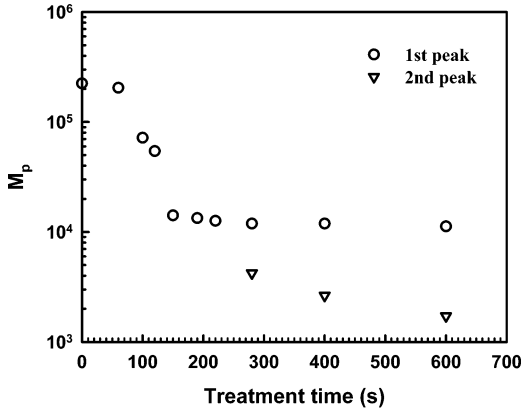

(a)

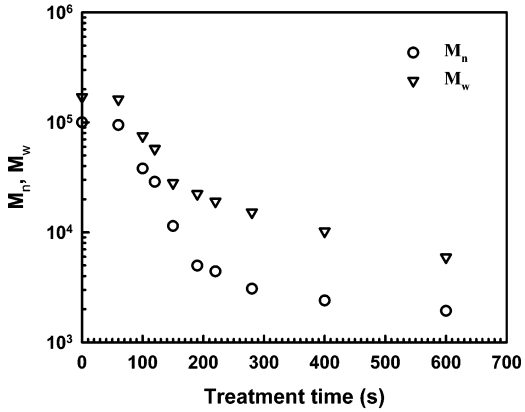

(b)

Figure 9. Change of molecular weight of Kraton 1107 as a function of heat treatment time: (a) peak molecular weights and (b) weight-average and number-average molecular weight calculated based on polystyrene standards. The annealing temperature is 160 °C.

time t, respectively. Evidently, eq 1 is deficient for Kraton 1107 because chain scission does not occur in the polystyrene block. Since polystyrene accounts only about 15% of the total molar mass of Kraton 1107, one may calculate the number-average degree of polymerization of isoprene segment by subtracting the molecular weight of polystyrene block as

$$\bar{X}_t = 0.85(M_n)_t/68.12 \qquad (2)$$

where 0.85 is the molar mass fraction of isoprene block at the onset of the reaction and 68.12 is the molecular weight of isoprene repeat unit. Strictly speaking, eq 2 is valid only at the early stage of decomposition. Note also that the number-average degree of polymerization is determined mainly by the low molar mass fractions, which are predominantly short oxidized polyisoprene chains, particularly at longer heat treatment time. As a result, the approximate N_S values may be computed from the number-average molecular weight in Table 1. Plots of N_S and $\bar{X}_t$ of isoprene segments in Kraton 1107 as a function of heat treatment time are depicted in Figure 10. After the induction period of 60 s, the chain scission event per unit isoprene chain accelerates, and concurrently the number-average molecular weight drastically declines and levels off after 200 s. The degradation is believed to occur in the styrene blocks as the styrene chains are thermally stable. The overall reduction in the molecular weight may be attributed to

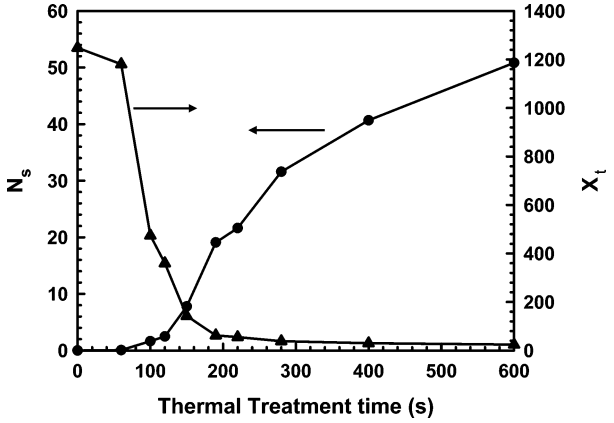

Figure 10. Average number of chain scission events and number-average degree of polymerization of isoprene segment in Kraton 1107 at 160 °C.

the detachment of the isoprene units from the copolymer as well as the reduction in molecular weight of the isoprene chains. After 200 s, the reaction event per isoprene chains continues to rise, which may be simply due to the continued decline of the number-average molecular weight, although it seems the molecular weight asymptotically levels off. There is a possibility that the increase in the functional groups due to the side reactions[21−27] such as formation of epoxy, peroxide, and hydroxide in the isoprene backbone may have expedited the reaction.

Such chemical modification may also have altered thermodynamic stability (or miscibility) with the SI copolymer containing short isoprene segments, which in turn drives the system to the unstable region again. Moreover, the continued detachment of isoprene units from the oxidized copolymer into nearly neat polystyrene and polyisoprene further reduces the compatibilizing effect, thereby promoting the macrophase separation. It is worth noting that the cascading phase separation appears heterogeneous, undergoing phase segregation within the preexisting domains as well as in the matrix. Hence, the second phase separation probably arises from the miscibility reduction between the nearly neat polystyrene and the heavily oxidized isoprene derivatives. The continued morphology evolution from 190 to 700 s is further affected by the oxidation (or functionalization), altering the chemical structure of the low molecular weight polyisoprene chains, which in turn changes the thermodynamic balance between the styrene and the isoprene chains.

Conclusions

In summary, when the SIS triblock undergoes thermooxidative degradation, it has broken down to two SI diblocks of different lengths and block ratios. With continued reaction, the SI diblock chains are chopped into low molecular weight polyisoprene and SI diblocks attached with short isoprene fragments. Because of the immiscibility of the styrene-rich SI copolymer and low molecular weight polyisoprene, macroscopic phase separation is believed to occur between the degrading polyisoprene and the SI diblock with shorten isoprene segments. This stage represents the first phase separation. The progressive decline of the molecular weight of the polyisoprene units further drives the immiscibility gap to a lower temperature, which tends to make the system to homogenize. This stage corresponds to the

phase dissolution, which presumably occurs in competition with the first phase separation especially at a lower reaction temperature, e.g., 150 °C. In the prolonged heating, secondary reactions such as chemical modification (or oxidation) occur in polyisoprene backbones that drive the system to be unstable, causing the second phase separation. It should be emphasized that, unlike the styrene-*block*-butadiene-*block*-styrene copolymers, there is essentially no cross-linking reaction in the thermal oxidation of styrene-*block*-isoprene-*block*-styrene copolymer.

Acknowledgment. Support of this work by Civilian Research and Development Foundation (CRDF) Award RC2-2398-MO-02 is gratefully acknowledged. We thank our Russian colleagues Drs. L. I. Manevitch, A. N. Ivanova, and S. I. Kushanov for their constructive criticisms and suggestions during T. Kyu's visit to Moscow.

References and Notes

(1) Molau, G. E. Colloidal and Morphological Behavior of Block and Graft Copolymers. In *Block Polymers*; Aggarwal, S. L., Ed.; Plenum Press: New York, 1970.
(2) Hashimoto, T. In *Thermoplastic Elastomers*, 1st ed.; Legge, N. R., Holden, G. R., Schroeder, H. E., Eds.; Hanser: Vienna, 1987; Chapter 12.
(3) Bates, F. S.; Fredrickson, G. H. *Annu. Rev. Phys. Chem.* **1990**, *41*, 525.
(4) Thomas, E. L.; Alward, D. B.; Kinning, D. J.; Martin, D. C.; Handling, D. C.; Fetters, L. J. *Macromolecules* **1986**, *19*, 2197.
(5) Hasegawa, H.; Tanaka, H.; Yamazaki, K.; Hashimoto, T. *Macromolecules* **1987**, *20*, 1651.
(6) Rösler, A.; Vandermeulen, G. W. M.; Klok, H.-A. *Adv. Drug Delivery Rev.* **2001**, *53*, 95.
(7) Moffitt, M.; Khougaz, K.; Eisenberg, A. *Acc. Chem. Res.* **1996**, *29*, 95.
(8) Dormidontova, E. E.; Lodge, T. P. *Macromolecules* **2001**, *34*, 9143.
(9) Scott, G. *Atmospheric Oxidation and Antioxidants*; Elsevier: London, 1965.
(10) Grassie, N.; Scott, G. *Polymer Degradation & Stabilisation*; Cambridge University Press: Cambridge, 1985.
(11) Allen, N. S.; Edge, M. *Fundamentals of Polymer Degradation and Stabilisation*; Elsevier Applied Science: London, 1992.
(12) Billingham, N. C. The Physical Chemistry of Polymer Oxidation and Stabilization. In *Atmospheric Oxidation and Antioxidants*; Scott, G., Ed.; Elsevier: Amsterdam, 1993; Vol. II, Chapter 4.
(13) Bevilacqua, E. M. Thermal and Oxidative Degradation of Natural Rubber and Allied Substances. In *Thermal Stability of Polymers*; Conley, R. T., Ed.; Marcel Dekker: New York, 1970; Vol. 1, Chapter 7.
(14) Kubo, J.; Onzuka, H.; Akiba, M. *Polym. Degrad. Stab.* **1994**, *45*, 27.
(15) Roe, R.-J.; Zin, W.-C. *Macromolecules* **1980**, *13*, 1221.
(16) Sung, L.; Han, C. C. *J. Polym. Sci., Part B: Polym. Phys.* **1995**, *33*, 2405.
(17) Han, C. D.; Kim, J.; Kim, J. K. *Macromolecules* **1989**, *22*, 383.
(18) Fan, S.; Kyu, T. *Macromolecules* **2000**, *33*, 9568; *Macromolecules* **2001**, *34*, 645; *Macromolecules* **2001**, *34*, 3790.
(19) Kim, J. Y.; Cho, C. H.; Palffy-Muhoray, P.; Mustafa, M.; Kyu, T. *Phys. Rev. Lett.* **1993**, *71*, 2232.
(20) Gunton, J. D.; San Miguel; Sahni, P. S. The Dynamics of First-Order Phase Transitions. In *Phase Transitions and Critical Phenomena*; Domb, C., Lebowitz, J. L., Eds.; Academic Press: New York, 1980; Vol. 8, pp 269−466.
(21) Golub, M. A.; Hsu, M. S.; Wilson, L. A. *Rubber Chem. Technol.* **1975**, *48*, 953.
(22) Bolland, J. L. *Trans. Faraday Soc.* **1950**, *46*, 358.
(23) Bevilacqua, E. M. *J. Am. Chem. Soc.* **1955**, *77*, 5394; *J. Am. Chem. Soc.* **1957**, *79*, 2915; *J. Polym. Sci.* **1961**, *49*, 495.
(24) Norling, P. M.; Lee, T. C. P.; Tobolsky, A. V. *Rubber Chem. Technol.* **1965**, *38*, 1198.
(25) Morland, J. L. *Rubber Chem. Technol.* **1977**, *50*, 373.
(26) Zhang, Y.; Wiesner, U.; Yang, Y.; Pakula, T.; Spiess, H. W. *Macromolecules* **1996**, *29*, 5427.
(27) Dalnoki-Veress, K.; Forrest, J. A.; Stevens, J. R.; Dutcher, J. R. *J. Polym. Sci., Part B: Polym. Phys.* **1996**, *34*, 3017.

MA0355960